Journal of Sol-Gel Science and Technology (2024) 111:659–670
https://doi.org/10.1007/s10971-024-06430-9

ORIGINAL PAPER

# Boosting the collapse performance of Wax-binder-free silica based ceramic core via adding nano-alumina sol modified fused silica powder

Yi Qin[1] · Xinsheng Sun[1] · Yani Cheng[1] · Lunkai Shi[1] · Zixu Wang[1] · Zhihao Qi[1] · Yuan Fang[1] · Jianfeng Zhu[1] · Ting Zhao[1]

Received: 8 January 2024 / Accepted: 21 May 2024 / Published online: 20 June 2024


## Abstract

Wax-binder-free silica-based ceramic core with high collapsibility plays a critical role in precision casting. However, the collapse performance will dramatically reduce because the densification was induced by liquid phase sintering from the indispensable fused silica component, which makes the core hard to be removed by mechanical vibration, especially for the semi-enclosed parts. Herein, we propose a liquid phase sintering restraint strategy for improving collapsibility by adding surface-modified fused silica powder. The results show that a high-temperature resistant alumina/mullite shell can be formed by pre-coating alumina sol on the surface of fused silica powder after the processing of preheating and casting. Compared with utilizing pure fused silica powder, when adding 25 wt% modified fused silica substituted some part of pure fused silica, the flexural strength, porosity and bulk density of ceramic core reaches 5.95 MPa, 31.61% and 1.56 g/cm$^3$ respectively. These parameters completely satisfied the requirements of high collapsibility for casting, which is attributed to effectively inhibiting sintering and maintaining the porous structure by the alumina/mullite layer. Finally, the actual collapse experimental result shows that the cores can be completely removed through mechanical vibration lasting 30 min. This strategy offers a new method for improving the collapse properties of the wax-binder-free silica-based ceramic core by adding surface modified fused silica powder.

## Graphical Abstract

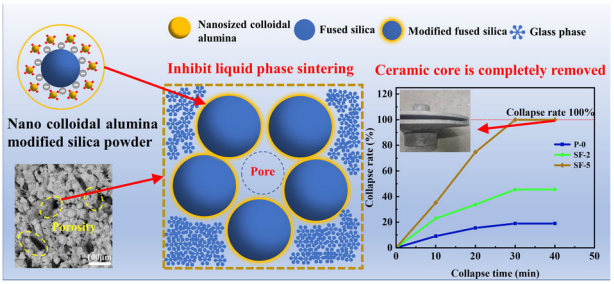


**Keywords** Silica-based ceramic cores · Porosity · Alumina/mullite coating · Collapse performance

✉ Ting Zhao
zhaoting@sust.edu.cn

[1] School of Materials Science and Engineering, Key Laboratory of Materials and Technology for Unearthed Cultural Heritage Conservation, Ministry of Education, Shaanxi Key Laboratory of Green Preparation and Functionalization for Inorganic Materials, Shaanxi University of Science and Technology, Xi'an 710021, China

**Highlights**

- Due to using inorganic binder sodium silicate, the preparation of wax-free silica-based ceramic cores was successfully achieved, and the sintering process did not require wax injection and wax removal.
- The synergistic effect of modified fused silica, cristobalite, and graphite formed a skeleton structure with high porosity inside the ceramic core.
- The addition of modified fused silica improved the collapse performance of silica-based ceramic cores by inhibiting liquid phase sintering.
- Based on the structural design, the ceramic core porosity was maintained at 31.61%, and the moderate flexural strength (5.95 MPa) was conducive to achieving 100% removal of the core only through mechanical vibration.

## 1 Introduction

Silica-based ceramic cores are widely used in the field of precision casting due to their excellent properties as a special structural material [1, 2]. In order to obtain high-quality products, extensive research has been undertaken into the production process of ceramic cores [3–5]. Ceramic cores must have sufficient flexural strength, high-temperature creep resistance, thermal expansion matching, chemical compatibility and collapse performance. As one of the complex problems in the study of ceramic cores, the collapse performance has attracted the attention of many researchers. Collapse performance mainly depends on porosity and improves with increasing porosity. The collapse of ceramic cores requires immersion in a leach solution, but the researchers found that the core removal process adversely affected the casting [6]. Therefore, it is essential to completely remove of the core while protecting the casting from being affected.

In our previous work, the effects of cristobalite addition on the crystallization, densification, mechanical, and collapse properties of the cores were systematically investigated [7]. According to reports, in order to further improve the collapse performance, the researchers adopted the method of adding sintering inhibitor [8–10] and pore-forming agent [11–13]. As a sintering inhibitor, cristobalite can be used as a seed crystal to change the initial temperature and promote crystallization. During the cooling stage, the phase transformation of cristobalite to tridymite will form micro-cracks in the core to improve the collapse performance. Graphite is a frequently used pore-forming agent that can increase the porosity of the core and significantly improve the collapse performance. If both cristobalite and graphite are added to the formula of the ceramic core, the ceramic core can be removed using only physical methods due to a combination of microcracks and pores. In contrast, the existence of microcracks and pores will reduce the mechanical properties of the ceramic core. How to guarantee that the ceramic core has the necessary mechanical properties and maximize its collapse performance is the key to this problem.

The modification of fused silica can significantly enhance the dispersion between $SiO_2$ particles and their compatibility with substances [14]. Furthermore, surface modification allows for coating the $SiO_2$ surface with active groups, effectively improving or controlling its surface activity [15–17]. This provides the possibility for ongoing grafting or functionalization of particles. The groups on the surface of $SiO_2$ can be physically modified or chemically modified. Common powder modifiers for physical modification include polymer and inorganic substances, which can effectively adsorb and change surface properties [18, 19]. The research [20] has found that the introduction of a core-shell structure is highly beneficial for enhancing the mechanical properties of the material, playing a significant role in both the "pinning effect" [21] and the "bridge effect" [22]. Cracks in the ceramic core matrix are influenced and either pinned or obstructed when passing through the core-shell particles. This results in a deviation from conventional transgranular fracture to a combined mode of transgranular and intergranular fracture [23]. For silica-based ceramic cores, synthesizing a nano-alumina coating on the surface of fused silica powder can effectively enhance the core's strength and resist crack propagation. However, the formation of the mullite phase during the casting process makes it more difficult for the ceramic core to dissolve in alkaline solutions, which does not improve leaching performance [24]. Based on this, modified fused silica is incorporated along with graphite and cristobalite. It is possible to enhance the strength of the ceramic core while maintaining its framework structure and porosity, thereby meeting the mechanical performance requirements of the ceramic core.

Hence, this research has presented a novel processing strategy to enhance the collapsibility of silica-based ceramic cores. We synthesize an alumina/mullite coating on the surface of fused silica powder to form a core-shell structure and add cristobalite and graphite to obtain a porous skeleton structure, which improves the collapse performance. The effects of different addition amounts of modified fused silica on the microstructure and mechanical properties of silica-based ceramic cores were investigated. The improvement in collapse performance eliminates the need for alkaline leaching of ceramic cores, aligning with the principles of green and sustainable development.

## 2 Methods

### 2.1 Preparation of modified fused silica

Fused $SiO_2$ powder coated with alumina/mullite was prepared by using molten $SiO_2$ powder and nano-colloidal $Al_2O_3$ as raw materials. First, an $Al_2O_3$ coating layer is prepared on the surface of molten $SiO_2$. Water molecules can be physically and chemically adsorbed on the surface of molten $SiO_2$, hydrolyzing the molten $SiO_2$ powder into substances with a large amount of [-OH]. In addition, H+ ions can be adsorbed on [-OH] on the surface of $Al_2O_3$ nanoparticles, making them positively charged. When 5 g of molten $SiO_2$ is added to $Al_2O_3$ nanoparticles in 100 ml of oxygen-containing acidic solution(water: alumina colloid = 1:1, pH ≈ 5) and stirred, the $SiO_2$ is covered by the $Al_2O_3$ adsorption layer due to the electrostatic attraction between opposite charges. After obtaining the $Al_2O_3$ nanoparticle coating layer, a high-temperature sintering method is used to prepare the alumina/mullite coating layer. After heating for 2 h at a sintering temperature exceeding 1300 °C, the molten $SiO_2$ surface reacts with the $Al_2O_3$ nanoparticles in situ to form a mullite phase and form a core-shell structure.

### 2.2 Preparation of ceramic core samples

$SiO_2$ powder with an average particle size of 30 μm (purity: 99.9%, Beijing Jingci New Material Technology Co., Ltd.) and 270 nm (purity: 99.9%, Beijing Jingci New Material Technology Co., Ltd., China) was selected as the basic component. In addition, graphite (30 μm purity: 99.9%, Beijing Jingci New Material Technology Co., Ltd.) was added as a pore-forming agent, cristobalite (100 μm, purity: 99.9%, Beijing Jingci New Material Technology Co., Ltd.) as a sintering inhibitor, and modified fused cristobalite to form the ceramic core formulation. The compositions of these materials are listed in Table 1, and the preparation process of the high-collapse silica-based ceramic cores is shown in Fig. 1. After mixing the raw materials evenly according to the formula, 4 wt% sodium silicate and 8 wt% water are stirred to form a slurry, and then the core is prepared by injection molding. It is sintered in a muffle furnace to 1200 °C and held for 1 h, then simulated casting at 1500 °C for 0.5 h.

### 2.3 Characterization

The phase composition and microstructure of $SiO_2$-based ceramic core materials were characterized by XRD (Smart Lab 9 kW, Rigaku Co., Ltd., Japan), scanning electron microscope (SEM, S8100, Hitachi Co., Ltd., Japan). The samples used for XRD analysis were all in block shape, with dimensions of approximately 15 × 12 × mm, and both sides were ground smooth. Crystallinity is calculated based on the position, number and relative intensity of the crystal diffraction peaks in the XRD pattern. The calculation formula is as follows:

$$X_c = \frac{I_c}{I_c + I_a} \times 100\% \quad (1)$$

where $X_c$ is the crystallinity (%) determined by X-ray diffraction; $I_c$ is the intensity of the crystalline diffraction peak; $I_a$ is the intensity of the non-crystalline dispersion peak.

Use a vernier caliper to measure the size of the sample after sintering, the accuracy is 0.01 mm, and the sample sintering shrinkage is calculated by the following formula (2):

$$S_L = \frac{L_0 - L_1}{L_0} \times 100\% \quad (2)$$

where $S_L$ is the sample sintering shrinkage (%); $L_0$ is the Sample length before sintering (mm); $L_1$ is the length of the sample after sintering (mm).

The bulk density and apparent porosity of the samples were determined by the Archimedes method and calculated according to formulas (3) and (4), respectively.

$$\rho_V = \frac{m_1}{m_3 - m_2} \times \rho_W \quad (3)$$

$$K_\alpha = \frac{m_3 - m_1}{m_3 - m_2} \times 100\% \quad (4)$$

where $\rho_V$ is the bulk density (g/cm$^3$); $K_\alpha$ is the apparent porosity (%); $m_1$ is the weight of the dry specimen (g); $m_2$ is the weight of the saturated specimen suspended and fully immersed in water (g); $m_3$ is the weight of sample in air when saturated (g); $\rho_W$ is the density of water at room temperature (g/cm$^3$).

The mechanical property was characterized by flexural strength, which was tested at room temperature by a

**Table 1** The ceramic core mixed powder composition(wt%)

| Sample | 30 μm $SiO_2$ powder | 270 nm $SiO_2$ powder | Modified fused $SiO_2$ | Cristobalite | graphite |
|---|---|---|---|---|---|
| P-0 | 75 | 25 | 0 | 0 | 0 |
| SF-1 | 60 | 25 | 15 | 0 | 0 |
| SF-2 | 30 | 25 | 45 | 0 | 0 |
| SF-3 | 0 | 25 | 75 | 0 | 0 |
| SF-4 | 30 | 25 | 15 | 20 | 10 |
| SF-5 | 30 | 25 | 25 | 10 | 10 |
| SF-6 | 30 | 25 | 35 | 0 | 10 |

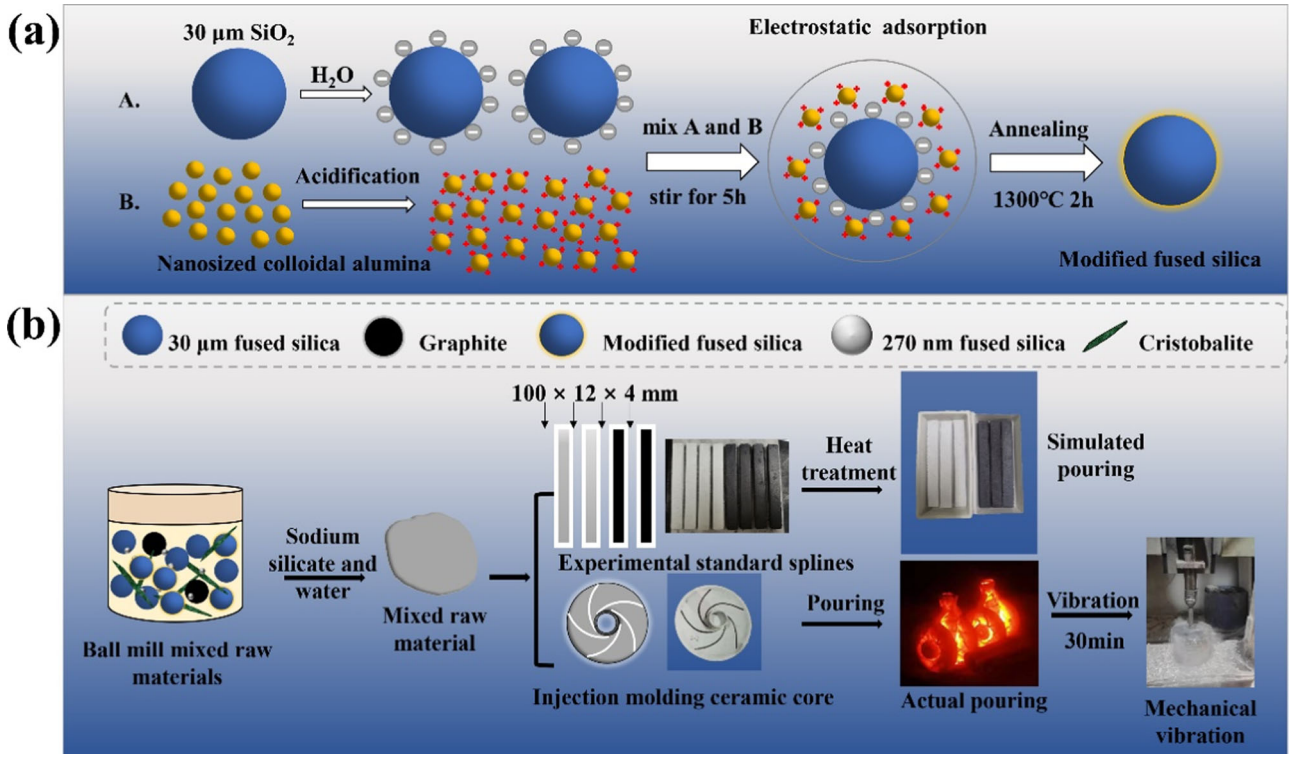


**Fig. 1** **a** Preparation technology of modified fused Silica; **b** Preparation process of the high collapse silica-based ceramic cores

universal testing machine (1036 PC, Taiwan Baoda Instrument Co., Ltd., China). The three-point bending strength was calculated according to formula (5), with a span of 30 mm and a loading rate of 1 mm/min. Each final value was averaged over five measurements, and the random errors were represented by standard deviations.

$$\sigma_\omega = \frac{3PL}{2bh^2} \tag{5}$$

where $\sigma_\omega$ is the flexural strength (MPa); $P$ is the load on the specimen at fracture (N); $L$ is the span between the two pivot points (mm); $b$ is the width of the specimen (mm); $h$ is the thickness of the specimen (mm).

In order to simulate specific industrial application conditions, the collapse characteristics of the sintered silica-based ceramic cores were investigated by using physical vibrations (Mechanical Vibrators, HZ-A, Xianxian Xusheng Construction Testing Instruments Co., Ltd., China). The weight loss of sintered silica-based ceramic cores for different physical vibrated times was tested. The calculation formula for the collapse rate is as follows:

$$\sigma_\omega = \frac{\Delta W}{W} \tag{6}$$

where $\sigma_\omega$ is the collapse rate (%); $\triangle W$ is the total weight loss (g); $W$ is the initial total weight (g).

## 3 Results and discussion

### 3.1 Characterization of modified fused silica powder

The XRD patterns and SEM images of the four raw materials of micron and nano-sized fused $SiO_2$ powders, cristobalite, and graphite are shown in Fig. 2. It can be seen that the silica particles exhibit spherical morphology at both particle sizes. Cristobalite and graphite powder have good crystallinity and irregular particles.

The XRD patterns, microscopic morphology images, EDX mapping and binary phase diagram of modified fused silica powder before and after high-temperature sintering are shown in Fig. 3. As shown in Fig. 3a, b, the particle surface becomes smoother after sintering at 1300 °C, indicating that the alumina coating on the surface of fused silica reacts with cristobalite to form the mullite phase. Meanwhile, the EDX results indicate that the sintered product is mainly composed of Si, Al and O, proving that the alumina/mullite coating was successfully formed.

### 3.2 Phase Composition of the silica-based ceramic cores

Silica-based ceramic cores with different amounts of modified fused silica were prepared according to the formula in

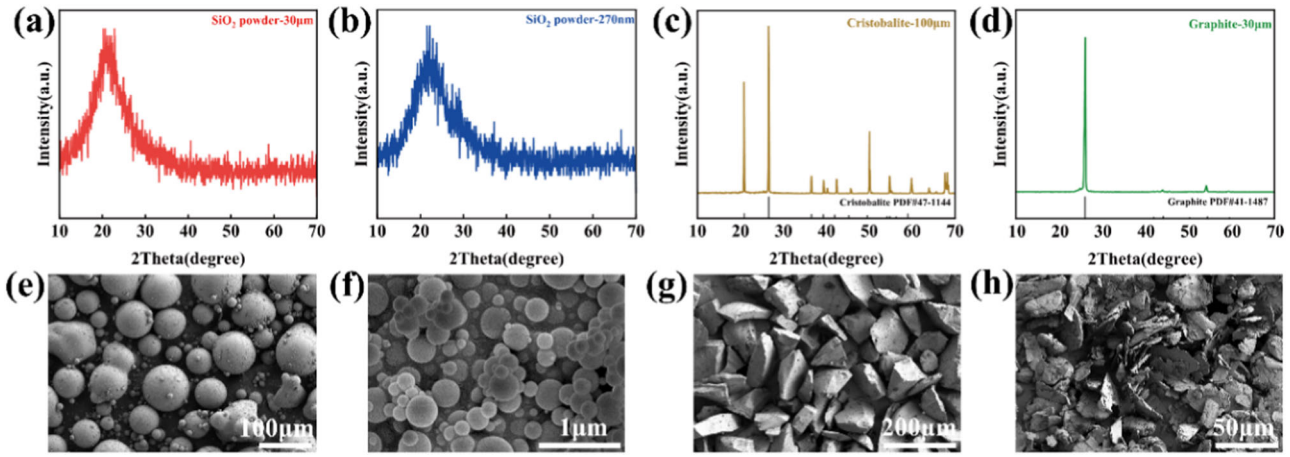


**Fig. 2** The phase composition and micromorphology of raw materials by XRD and SEM. (**a**, **e**), (**b**, **f**), (**c**, **g**) and (**d**, **h**) are 30 μm fused $SiO_2$ powder, 270 nm fused $SiO_2$ powder, cristobalite powder and graphite powder, respectively

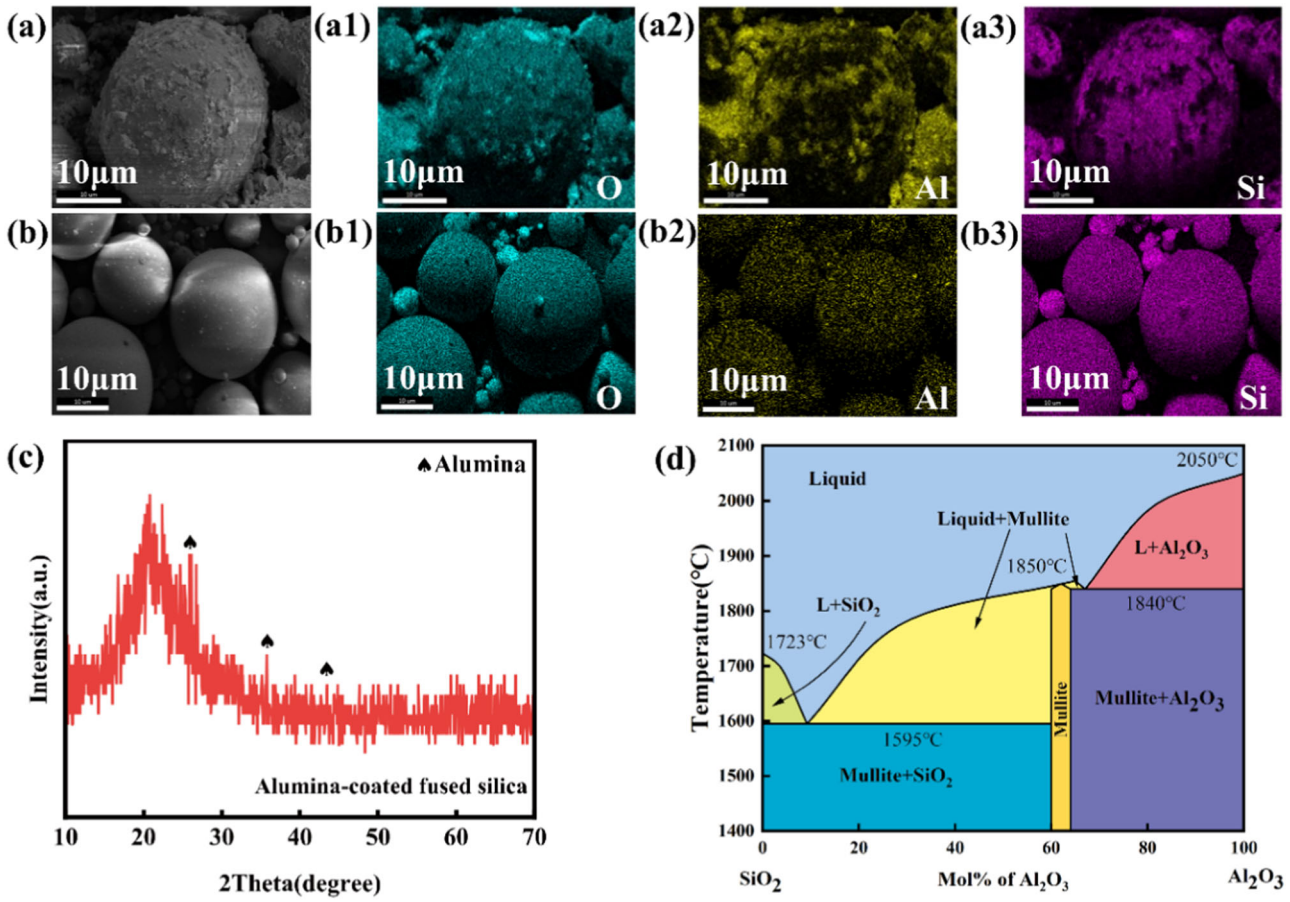


**Fig. 3** SEM images (**a**–**b**) and EDX mapping of O (**a1**–**b1**), Al (**a2**–**b2**) and Si(**a3**–**b3**) of modified fused silica powder before and after high-temperature sintering; (**c**) XRD pattern of modified fused silica; (**d**) binary phase diagram of alumina and silica [29]

Table 1. Figure 4a shows the XRD patterns of silica-based ceramic cores after sintering with different formulas. After adding modified fused silica, the cristobalite diffraction peak intensity of the sample decreased. Adding modified silica with alumina/mullite coating incorporates nano-alumina particles into the reaction system. As a result, cristobalite precipitates on the surface of fused silica and reacts with nano-alumina to form a mullite phase, which

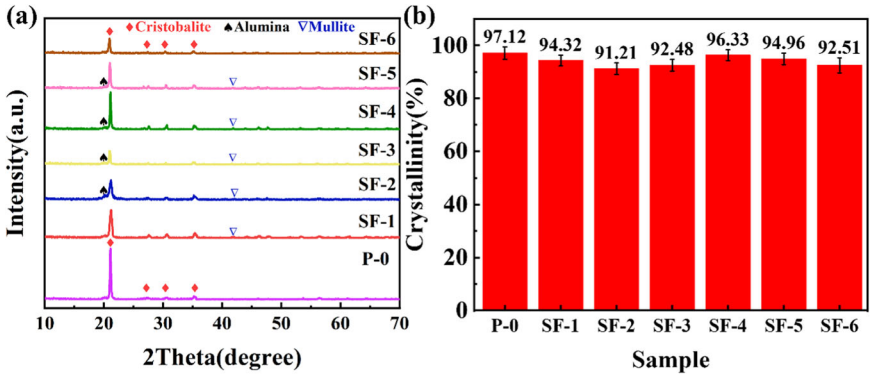


**Fig. 4** **a** XRD patterns of ceramic cores with different adding amount of modified fused silica after sintering at 1500 °C; **b** Crystalline phase contents of the ceramic cores

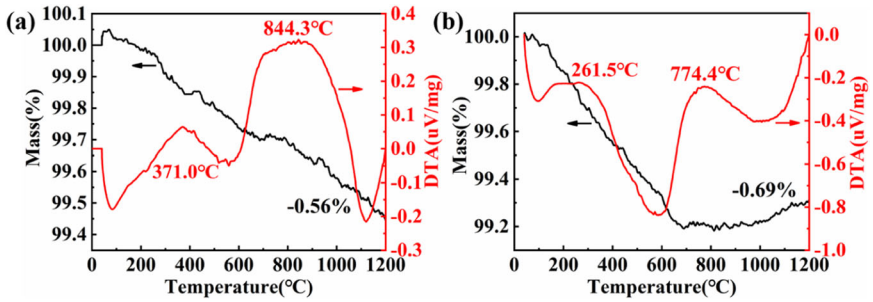


**Fig. 5** **a** TG-DTA curve of original formula(P-0); **b** TG-DTA curve of the formula added modified fused silica (SF-5)

reduces the content of cristobalite in the ceramic core [25]. Meanwhile, the intensity of the cristobalite diffraction peak in the ceramic core decreases simultaneously with the crystallinity, and a small number of diffraction peaks of alumina and mullite phases are observed. It is also noteworthy that when cristobalite and modified fused silica are added simultaneously to the formulation, the diffraction peak intensity of the cristobalite increases as the additional cristobalite induces crystallization. The modified fused silica is composed of silica surrounded by alumina/mullite shells and has a higher crystalline phase content. In particular, the relative crystallinity of the SF-4 sample reaches 96.33%.

For studying the effect of adding modified fused silica on the ceramic cores, Fig. 5 shows the comparison of TG-DTA curves before and after adding modified fused silica. Compared with the original formulation (P-0), the addition of modified fused silica to the sample resulted in a decrease in the phase transition temperature from 844.3 °C to 774.4 °C, indicating that the alumina/mullite coating reduced the phase transition temperature. The exothermic peak at 261.5 °C is the weight loss process of the ceramic core. An endothermic peak is observed at 600 °C, which is attributed to the formation of cristobalite. The transition temperature of the fused silica ceramic core increases the rate of transition from fused silica to cristobalite. Cristobalite precipitates on the surface of silica, inhibiting the mass transfer process and hindering sintering densification.

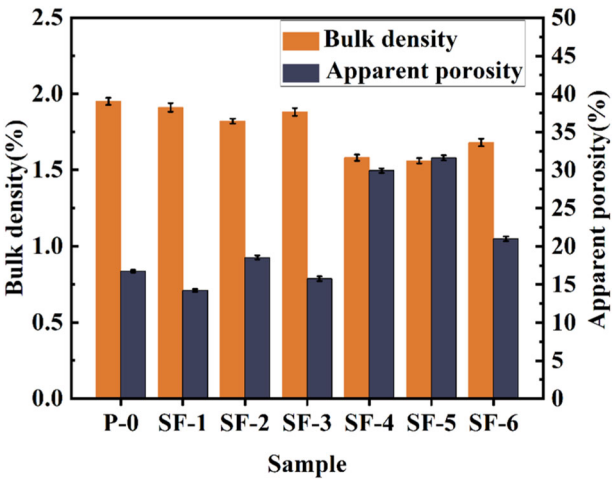


**Fig. 6** Bulk densities and apparent porosities of the ceramic cores with different adding amount of modified fused silica

### 3.3 Porosities of the silica-based ceramic cores

In order to quantify the effect of varying amounts of modified fused silica on the densification of the silica-based ceramic core during sintering, Fig. 6 shows the variation of bulk density and apparent porosity of the silica-based ceramic cores with different addition amounts of modified fused silica. For samples SF-1, SF-2 and SF-3, when the additional amount of modified fused

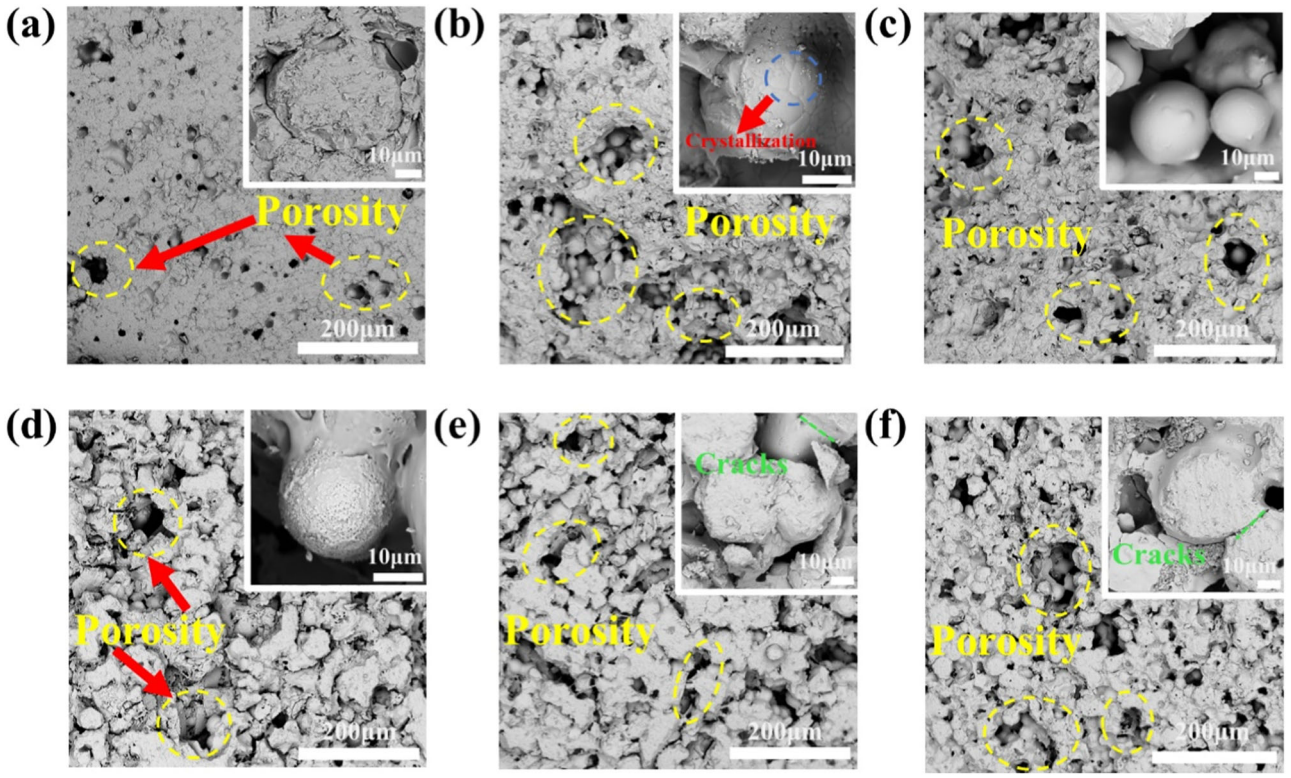


**Fig. 7** The SEM images in BS mode of ceramic cores with different adding amount of modified fused silica after sintering at 1500 °C. **a** SF-1; (**b**) SF-2; (**c**) SF-3; (**d**) SF-4; (**e**) SF-5; (**f**) SF-6

silica is 45 wt% (SF-2), the minimum packing density of the ceramic core is 1.82 g/cm$^3$ and the porosity is 18.55%. For the SF-4, SF-5 and SF-6 samples, the incorporation of cristobalite and graphite significantly increased the porosity of the ceramic core. When the additional amount of modified fused silica is 25 wt% (SF-5), the minimum packing density of the ceramic core is 1.56 g/cm$^3$, and the porosity is 31.61%. It has been reported that the porosity of typical silica-based ceramic cores is less than 35%, and high porosity is beneficial to the collapse of the core [26]. The liquid-phase adhesion of the nano-alumina coating incorporated by modified fused silica hinders the liquid-phase movement between silica particles, thereby increasing the porosity of the ceramic core. On the other hand, the addition of cristobalite as a heterogeneous nucleating agent will induce crystallization and hinder the sintering process. Therefore, the ceramic core porosity increases. However, the mullite phase generated by the reaction between alumina and cristobalite on the surface of modified fused silica is a low melting point liquid phase. The liquid phase fills part of the pores during its movement and causes a decrease in porosity. Although adding cristobalite can improve silica ceramic cores' porosity, excess cristobalite may weaken this improvement. Consequently, the addition of 25wt% modified fused silica (SF-5) is conducive to obtaining the best porosity of the silica ceramic core.

The microstructure changes of silica-based ceramic core materials with different amounts of modified fused silica were compared through BS mode of SEM. As shown in Fig. 7, the microstructure of the ceramic core used large particles fused silica crystal as a framework and small particles were dispersed in the matrix to connect the particles. Some open pores and closed pores can be observed on the surface of the ceramic core, and the morphology changes are consistent with the porosity change trend. For samples SF-1, SF-2 and SF-3, as the amount of modified fused silica increases, the structure is the loosest when the addition amount is 45 wt%. For samples SF-4, SF-5 and SF-6, when the additional amount of modified fused silica reaches 25 wt% (SF-5), the surface micropores are the most. On the one hand, the addition of cristobalite and graphite effectively improves the micromorphology of the ceramic core surface. On the other hand, the liquid phase adhesion of modified fused silica particles inhibits liquid phase sintering and increases the porosity of the ceramic core. In Fig. 7e, f, there is an apparent liquid phase coating on the particle surface, which proves that the alumina/mullite coating causes liquid phase adhesion to prevent the liquid phase from filling the pores. As the additional amount of modified fused silica increases,

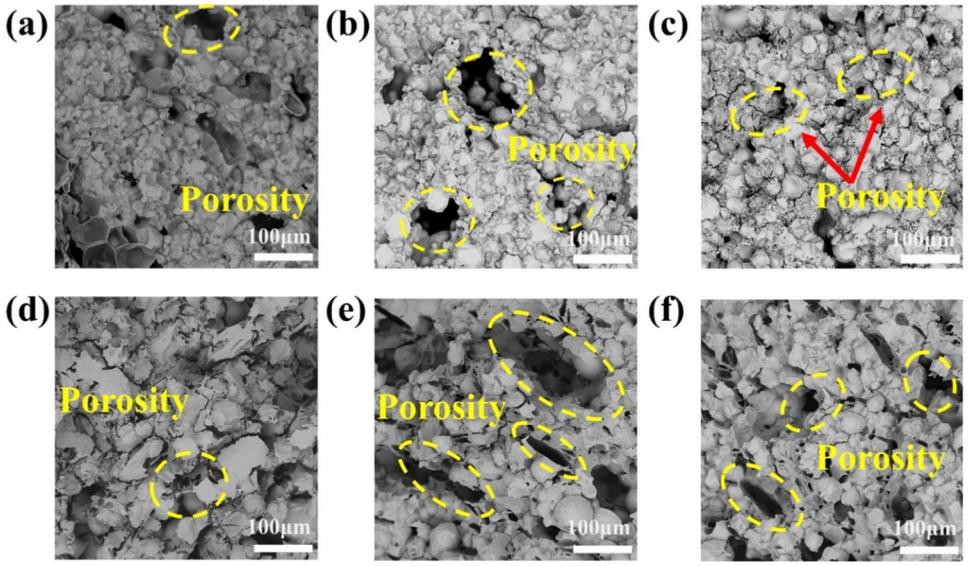


**Fig. 8** SEM images of the fracture surfaces of ceramic cores with different adding amount of modified fused silica after sintering at 1500 °C. **a** SF-1; (**b**) SF-2; (**c**) SF-3; (**d**) SF-4; (**e**) SF-5; (**f**) SF-6

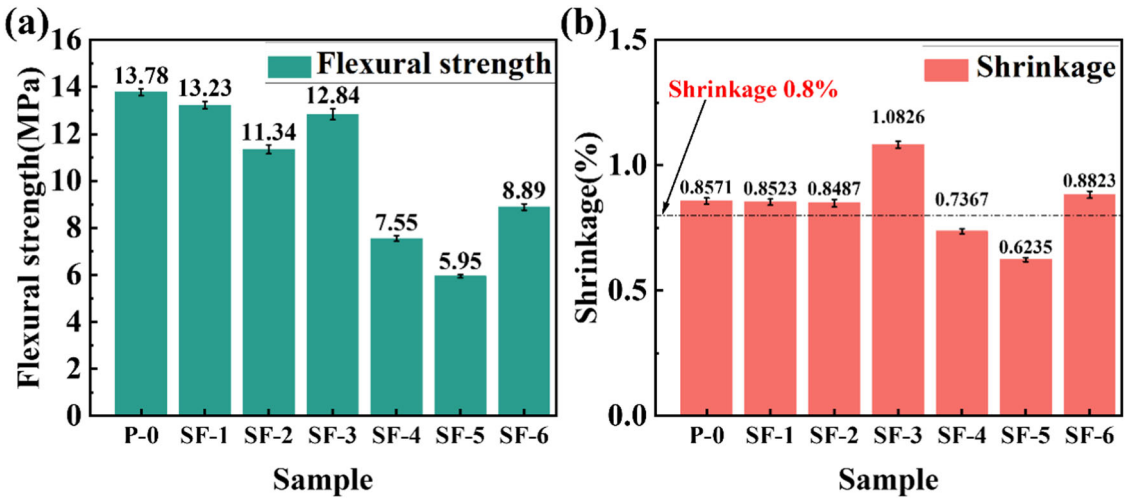


**Fig. 9** **a** Flexural strength of ceramic cores with different adding amount of modified fused silica; (**b**) Shrinkage of ceramic cores with different adding amount of modified fused silica

the particle size does not change significantly, but the porosity increases significantly.

In order to further observe the microstructure inside the ceramic core, the structural changes after the porosity change were verified. The SEM images of the fracture surfaces of ceramic cores with different compositions after final sintering at 1500 °C are shown in Fig. 8. The particles on the surface of the fracture in the figure are complete, many small powder particles surround large powder particles, and irregular particles remain in the sintered body. On the other hand, the precipitated cristobalite undergoes a phase transformation from β-cristobalite to α-cristobalite during the reaction, which results in a 5% volume reduction and the extension of microcracks in the ceramic core. Furthermore, many narrow and long micropores are observed in Fig. 8d–f. The micropores formed by these will destroy the internal structure of the ceramic core and increase the possibility of mechanical vibration to remove the silica-based ceramic core.

### 3.4 Mechanical performance of the silica-based ceramic cores

The mechanical properties of the silica-based ceramic core are related to whether the ceramic core can be easily removed by mechanical vibration while maintaining the essential strength. Figure 9a shows the flexural strength of ceramic cores with different formulas at room temperature. For the SF-1, SF-2 and SF-3 samples, as the addition of modified fused silica increases to 75 wt% (the fused silica is completely replaced), the flexural strength of the ceramic core first decreases and then increases. When the additional

amount of modified fused silica reaches 45 wt%, the minimum flexural strength is 11.34 MPa. The minimum flexural strength for the SF-4, SF-5 and SF-6 samples was 5.95 MPa when the additional amount of modified fused silica reached 25 wt%. The main reason for the decrease in flexural strength is that adding cristobalite and graphite builds a loose and porous skeleton inside the ceramic core. The combined effect of micropores and microcracks reduces the flexural strength of the ceramic core. On the other hand, the formation process of the mullite phase reduces the alumina and cristobalite content in the core material. As the two main reinforcing phases in ceramic cores, reducing their content will decrease the core's flexural strength. However, the alumina/mullite coating can prevent crack propagation on the silica surface, and adding excess amounts of modified fused silica will reduce the core's porosity. Therefore, under the high addition amount of modified fused silica, the flexural strength of the ceramic core has a slight rebound. The SF-5 formula has the lowest flexural strength and can meet the mechanical performance requirements for ceramic cores, which is conducive to the collapse of ceramic cores.

Figure 9b shows the shrinkage rate of silica-based ceramic cores with different amounts of modified fused silica. The ceramic core shrinkage rates are around 0.8%, meeting the performance requirements [27]. For the SF-1, SF-2 and SF-3 samples, when the modified fused silica is used as a complete replacement for fused silica (75 wt%), the shrinkage initially decreases and then increases. For the three groups of formulations adding cristobalite (0–20 wt%) and graphite (10 wt%), the shrinkage rate is as low as 0.62% when the modified fused silica addition is 25 wt%. The main reason for the change in shrinkage is the volume effect caused by the crystalline transformation of cristobalite and the volume shrinkage caused by the densification of the core during the sintering process. Notably, the abnormally increased shrinkage in Fig. 9b could be attributed to the increase in the percentage of glass phase in the specimen during the simulated casting process. When the liquid phase wets the surface of a solid powder, the distance between the powder particles is reduced due to the surface tension of the liquid phase. Therefore, the shrinkage rate of the specimen suddenly changes. The shrinkage rate of ceramic cores for all formulas mainly stayed the same, meeting the requirements for the use of ceramic cores.

## 3.5 Collapse performance of the silica-based ceramic cores

Figure 10 shows the collapse performance of the silica-based ceramic core. Three core formulas(P-0, SF-2, SF-5) were selected to observe the collapse process of the ceramic core through mechanical vibration. The weight loss of the ceramic core gradually increases with the increase of the mechanical vibration time. After 30 min of mechanical vibration, the core of the casting inner cavity no longer loses weight. The results show that only 18.96% of the ceramic core with the P-0 formula was slowly removed through mechanical vibration. In contrast, the ceramic core with the SF-5 formula completely fell off after 30 min of vibration. A collapse rate of up to 100% means that the silica-based ceramic core of the SF-5 formula has good collapse performance.

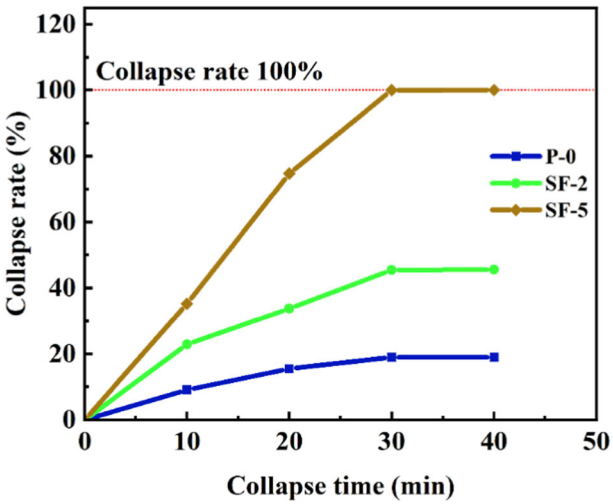


**Fig. 10** The collapse rate of ceramic cores with different adding amount of modified fused silica

In order to better prove the excellent collapse performance of the modified ceramic core, Fig. 11 shows the optical photos of the ceramic core (a) and the photo of metal parts cast with ceramic cores prepared by P-0 and SF-5 formula (b). After 30 min of mechanical vibration, the collapse rate of the core is shown in Fig. 11c, d. Compared with the unmodified P-0 formula, the SF-5 formula has better collapse performance. Metal castings cast with SF-5 ceramic cores have no core residue inside, and the collapse rate is as high as 100%.

## 3.6 The action mechanism of modified fused silica

The action mechanism diagram of modified fused silica is shown in Fig. 12. The coated fused silica particles form a "core-shell" structure that inhibits the coarsening of the sintering neck, and the alumina/mullite coating forms a barrier layer that inhibits liquid-phase sintering of the core. It is known that the diffusion activation energy of alumina is higher than that of fused silica, so it is difficult for the coated fused silica particles to form sintering necks through surface diffusion. Furthermore, the alumina/mullite coating forms a barrier layer that impedes liquid phase movement between the coated fused silica particles, thus preventing the pore-filling process. According to the powder sintering

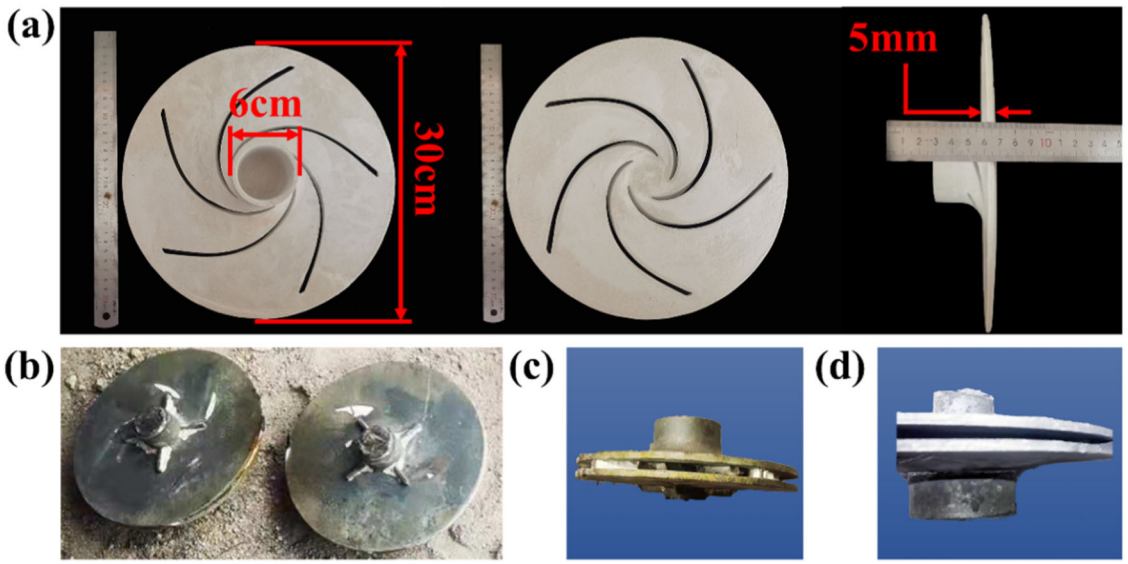


**Fig. 11** **a** Optical photos of the front, back and side of the ceramic core after sintering; **b** The photo of metal parts cast with ceramic cores prepared by P-0 and SF-5 formula; **c** Ceramic core after mechanical vibration (P-0); **d** Ceramic core after mechanical vibration (SF-5)

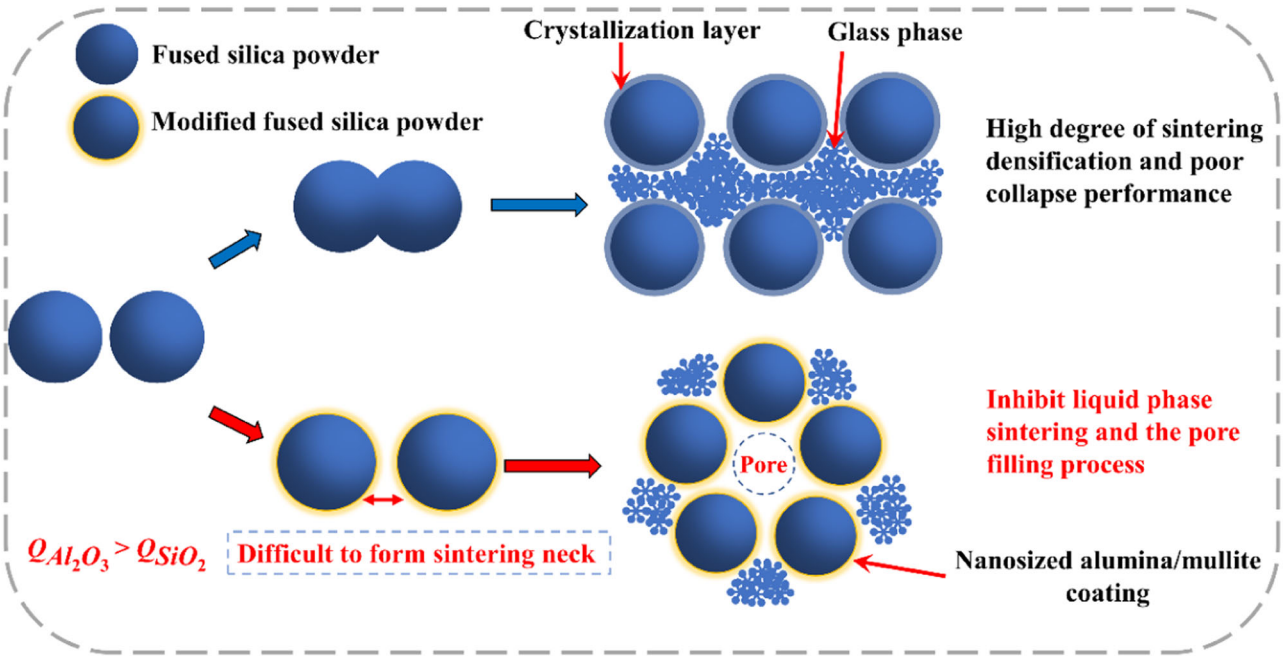


**Fig. 12** The mechanism diagram of modified fused silica

theory, as the particle size of the powder particles becomes smaller, the adhesion effect will become stronger. This adhesion is an essential factor in the bonding, aggregation and rearrangement between powder particles during the sintering stage. As the amount of modified fused silica increases, the porosity, shrinkage and flexural strength of the ceramic core change uniformly. The alumina/mullite coating inhibits the tendency of the liquid phase to fill the pores and increases the viscosity of the system. As the porosity increases, the flexural strength decreases. As the content of modified fused silica further increases, the content of fused silica decreases relatively, and sufficient alumina enters the system to react with silica to form a low melting point liquid phase ($3Al_2O_3{\cdot}2SiO_2$). The formation of the mullite phase increases the liquid phase in the sintered sample content, porosity is reduced, and the flexural

strength is slightly increased. Therefore, the additional amount of modified fused silica should not be excessive, and the appropriate addition amount (25 wt%) is enough to improve the collapse performance of the silica-based ceramic core. The inhibition of microcrack propagation by the alumina/mullite coating also increases the flexural strength of the core [28]. The binary phase diagram of alumina and silica is shown in Fig. 3d. The main shrinkage process of the core is divided into two stages: the heating stage (1100–1550 °C) and the cooling stage (200–300 °C). The first stage may be related to shrinkage caused by densification of the specimen during sintering. The second shrinkage stage may correspond to the phase transformation of β-cristobalite to α-cristobalite during cooling, resulting in a volume change of approximately 5%. The most important shrinkage occurs in the first stage (heating). The combined effect of micropores and microcracks can effectively improve the collapse performance of the silica-based ceramic core. Therefore, after simple mechanical vibration, the inner wall ceramic core of the metal casting is completely removed without residue and without alkali boiling.

## 4 Conclusions

In this study, we present a novel strategy a novel strategy to prepare high-collapse silica-based ceramic cores successfully. Experimental results show that surface modification of fused silica powder and the addition of pore-forming agents and sintering inhibitors greatly improve the collapse performance of silica-based ceramic cores. At the same time, it meets the mechanical performance requirements for the use of ceramic cores. Furthermore, we systematically investigated the effects of modified fused silica addition on the crystallization, densification, mechanical and collapse properties of the ceramic cores. When the modified fused silica addition reached 25 wt%, the porosity reached as high as 31.61%, and the flexural strength was only 5.95 MPa. After 30 min of mechanical vibration, the core collapse rate reached 100%. The successful preparation of high collapse silica ceramic cores without wax removal is expected to reduce the damage to castings and core residues during the core collapse process and promote the wider application of silica-based ceramic cores in precision casting.

**Acknowledgements** This work was grateful with the support of the National Natural Science Foundation of China [Grant No. 51702193], the Natural Science Basic Research Program of Shaanxi [Grant No. 2022JM-202, 2022JM-285], the Key Scientific Research Program of Shaanxi Province Education Department [No. 23JY010], the Shaanxi Provincial Education Department serves Local Scientific Research Plan [Grant No. 20JC008], the General Project in Industrial Area of Shaanxi Province [Grant No. 2020GY-281] and the Scientific Research Fund of Shaanxi University of Science & Technology [Grant No. BJ16-20, BJ16-21].

**Author contributions** Yi Qin: conceptualization, formal analysis, validation, investigation, data curation, writing-original draft. Ting Zhao: data curation, supervision, writing-review & editing. Xinsheng Sun: resources, validation. Yani Cheng: investigation, validation. Lunkai Shi, Zixu Wang, and Zhihao Qi: formal analysis. Yuan Fang and Jianfeng Zhu: data curation.

## Compliance with ethical standards

**Conflict of interest** The authors declare no competing interests.

## References

1. Ozkan B, Sameni F, Goulas A, Karmel S, Engstrøm DS, Sabet E (2022) Hot ceramic lithography of silica-based ceramic cores: The effect of process temperature on vat-photopolymierisation. Addit Manuf 58:103033
2. Li X, Niu S, Wang D, Li J, Jiao Q, Guo X, Xu X (2023) Microstructure and crystallization kinetics of silica-based ceramic cores with enhanced high-temperature property. Materials 16:606
3. Xu X, Niu S, Wang X, Li X, Li H, Su X, Luo S (2019) Fabrication and casting simulation of composite ceramic cores with silica nanopowders. Ceram Int 45:19283–19288
4. Ackley BJ, Martin KL, Key TS, Clarkson CM, Bowen JJ, Posey ND, Ponder Jr JF, Apostolov ZD, Cinibulk MK, Pruyn TL (2023) Advances in the synthesis of preceramic polymers for the formation of silicon-based and ultrahigh-temperature non-oxide ceramics. Chem Rev 123:4188–4236
5. Yng K, Li Q, Chen T, Jin F, Liu X, Liang J, Li JG (2023) High-performance 3D-printed $Al_2O_3$ cores for low-temperature sintering. Ceram Int 49:36894–36906
6. Yang Z, Li K, Ma S, Yu J, Ren Z (2021) Preparation, mechanical, and leaching properties of $CaZrO_3$ ceramic cores. Int J Appl Ceram Technol 18:1490–1497
7. Qin Y, Cheng Y, Li J, Zhang H, Zhu J, Zhao T (2023) Improved collapse properties of silica-based ceramic cores via flexibly regulating cristobalite content. Int J Appl Ceram Technol 20:3666–3676
8. Breneman RC, Halloran JW, Sglavo V (2015) Effect of cristobalite on the strength of sintered fused silica above and below the cristobalite transformation. J Am Ceram Soc 98:1611–1617
9. Kazemi A, Faghihi-Sani MA, Alizadeh HR (2013) Investigation on cristobalite crystallization in silica-based ceramic cores for investment casting. J Eur Ceram Soc 33:3397–3402
10. Yin Y, Wang J, Huang Q, Xu S, Shuai S, Hu T, Xuan W, Yin S, Chen C, Ren Z (2023) Influence of debinding parameter and nano-ZrO2 particles on the silica-based ceramic cores fabricated by stereolithography-based additive manufacturing. Ceram Int 49:20878–20889
11. Tang S, Yang L, Li G, Liu X, Fan Z (2018) Fabrication of ceramic cores via layered extrusion forming using graphite as pore-forming agent. IOP Conf Ser Mater Sci Eng 423:012065
12. Liu S, Zeng Y, Jiang D (2009) Fabrication and characterization of cordierite-bonded porous SiC ceramics. Ceram Int 35:597–602
13. Fang L, Chen C, Wang Y (2022) Carbon fibers and graphite as pore-forming agents for the obtention of porous alumina: correlating physical and fractal characteristics. Fractal Fract 6:501
14. Boyd DA, Frantz JA, Bayya SS, Busse LE, Kim W, Aggarwal I, Poutous M, Sanghera J (2016) Modification of nanostructured fused silica for use as superhydrophobic, IR-transmissive, anti-reflective surfaces. Opt Mater 54:195–199
15. Liang J, Lin Q, Zhang X, Jin T, Zhou YZ, Sun XF, Choi BG, Kim IS, Do JH, Jo CY (2017) Effects of alumina on cristobalite

crystallization and properties of silica-based ceramic cores. J Mater Sci Technol 33:204–209
16. Chen X, Liu C, Zheng W, Han J, Zhang L, Liu C (2020) High strength silica-based ceramics material for investment casting applications: Effects of adding nanosized alumina coatings. Ceram Int 46:196–203
17. Lu Z, Fan Y, Miao K, Jing H, Li D (2014) Effects of adding aluminum oxide or zirconium oxide fibers on ceramic molds for casting hollow turbine blades. Int J Adv Manuf Technol 72:873–880
18. Nayl A, Abd-Elhamid A, Aly AA, Bräse S (2022) Recent progress in the applications of silica-based nanoparticles. RSC Adv 12:13706–13726
19. Manyangadze M, Chikuruwo N, Chakra C, Narsaiah T, Radhakumari M, Danha G (2020) Enhancing adsorption capacity of nano-adsorbents via surface modification: a review. S Afr J Chem Eng 31:25–32
20. Bai X, Huang C, Wang J, Zou B, Liu H (2015) Fabrication and characterization of $Si_3N_4$ reinforced $Al_2O_3$-based ceramic tool materials,. Ceram Int 41:12798–12804
21. Liao M, Nicolini P, Du L, Yuan J, Wang S, Yu H, Tang J, Cheng P, Watanabe K, Taniguchi T (2022) UItra-low friction and edge-pinning effect in large-lattice-mismatch van der Waals heterostructures. Nat Mater 21:47–53
22. Hooper JB, Schweizer KS (2005) Contact aggregation, bridging, and steric stabilization in dense polymer-particle mixtures. Macromolecules 38:8858–8869
23. Huo M, Li Q, Liu J, Zhang X, Yue X, Liang J, Li J (2022) In-situ synthesis of high-performance $Al_2O_3$-based ceramic cores reinforced with core-shell structures. Ceram Int 48:33693–33703
24. Chen X, Zheng W, Zhang J, Liu C, Han J, Zhang L, Liu C (2020) Enhanced thermal properties of silica-based ceramic cores prepared by coating alumina/mullite on the surface of fused silica powders. Ceram Int 46:11819–11827
25. Li Q, Meng X, Zhang X, Liang J, Zhang C, Li J, Zhou Y, Sun X (2022) Enhanced 3D printed $Al_2O_3$ core via in-situ mullite. Addit Manuf 55:102826
26. Zhao Z, Yang Z, Yin Z, Chen B, Yu J, Ren Z, Yu H, Zhang G (2021) Physics, investigation of the properties and leaching characteristics of ceramic cores fabricated using $BaZrO_3$ as the raw material. Mater Chem Phys 272:124925
27. Hossain SS, Roy PK (2021) Preparation of multi-layered (dense-porous) lightweight magnesium-aluminum spinel refractory. Ceram Int 47:13216–13220
28. Dai Y, Yin Y, Xu X, Jin S, Li Y, Harmuth H (2018) Effect of the phase transformation on fracture behaviour of fused silica refractories. J Eur Ceram Soc 38:5601–5609
29. Aramaki S, Roy R (1962) Revised phase diagram for the system $Al_2O_3$-$SiO_2$. J Am Ceram Soc 45:229–242